Available online at www.sciencedirect.com
SCIENCE DIRECT®
Journal of Crystal Growth 267 (2004) 458–465
JOURNAL OF CRYSTAL GROWTH
www.elsevier.com/locate/jcrysgro

Relationship of growth mode to surface morphology and dark current in InAlAs/InGaAs avalanche photodiodes grown by MBE on InP

A.S. Huntington[a,b], C.S. Wang[c,*], X.G. Zheng[d], J.C. Campbell[d], L.A. Coldren[a,c]

[a] Department of Materials, University of California, Santa Barbara, Santa Barbara, CA 93106, USA
[b] Voxtel, Inc., Beaverton, OR 97005, USA
[c] Department of Electrical and Computer Engineering, University of California, Santa Barbara, Santa Barbara, CA 93106, USA
[d] Department of Electrical and Computer Engineering, The University of Texas, Austin, TX 78712, USA

Received 24 November 2003; accepted 20 April 2004

Communicated by D.W. Shaw

Abstract

We present the relationship between surface roughness and dark current measured for avalanche photodiodes with InGaAs absorbers and thin InAlAs multiplication layers fabricated from material grown lattice-matched to InP by molecular beam epitaxy. In particular, the leakage current at unity gain measured for sets of 125 μm diameter devices was found to have an exponential dependence upon the peak-to-peak surface roughness of the material, and was characterized by an order of magnitude increase for every 15 nm of roughness. We also present the results of an atomic force microscope study of surface morphology and growth conditions, interpreting the results in the context of diffusional versus convective growth modes. The best material was obtained at a substrate temperature of 500°C and an arsenic beam pressure of 8×10^{-6} Torr; the smooth growth window was bounded on the high-arsenic/low-temperature side by roughness resulting from low adatom surface mobility, and on the low-arsenic/high-temperature side by nonstoichiometric arsenic deficient growth.

Keywords: A1. Surface roughness; A3. Molecular beam epitaxy; B2. Semiconducting quaternary alloys; B3. Avalanche photodiodes

1. Introduction

We have previously reported molecular beam epitaxy (MBE)-grown avalanche photodiodes (APDs) with InGaAs absorbers and thin InAlAs multiplication layers fabricated in highly uniform 12×12 and 18×18 arrays [1,2]. We have also demonstrated individual devices which we believe to be the largest of their type yet reported (1 mm), and impact-ionization-engineered (I^2E) multiplication layers with extremely low excess noise [2,3]. Several growth attempts were necessary in each

*Corresponding author. Tel.: +1-805-893-7065; fax: +1-805-893-4500.
E-mail address: cswang@engineering.ucsb.edu (C.S. Wang).

0022-0248/$ - see front matter © 2004 Elsevier B.V. All rights reserved.
doi:10.1016/j.jcrysgro.2004.04.041

case to produce wafers suitable for the studies in question because of variations in device performance that were traced to run-to-run variations in material quality. In particular, it was empirically found that APDs fabricated from wafers with moderately rough surfaces tended to exhibit high dark leakage currents. Similar observations have been reported in the past relating interface morphology in heterostructures to optical and electronic properties, such as photoluminescence (PL) line width, electron mobility, and transport lifetimes [4–6]. This paper examines the impact of growth conditions upon wafer morphology and presents an empirical relationship between surface roughness and APD dark current.

1.1. Epitaxially-grown SACM APDs

The control over layer composition, thickness, and dopant density afforded by epitaxial growth allows several refinements of APD design that are not possible to implement in homojunction APDs formed by standard dopant diffusion techniques. The low bandgap material necessary to receive the long-wavelength (1310–1550 nm) light relevant to fiberoptic telecommunications is susceptible to leakage via interband tunneling when placed under strong bias. This source of dark current can be suppressed by isolating the low-bandgap material in a dedicated absorption layer in which the electric field is moderated by an adjacent charge layer: the separate absorption, charge, and multiplication (SACM) design, as diagramed in Fig. 1 [7]. SACM APDs can also be modulated faster than homojunction APDs because photogeneration of carriers is confined to a single layer, which shortens the impulse response of the detector [7,8]. A second advantage of epitaxial growth is the opportunity to engineer the multiplication layer so as to produce spatial correlations between impact ionization events, thereby suppressing multiplication noise [9,10]. However, these advanced designs typically involve multiplication layers on the order of 150–200 nm thick, supporting fields above 400 kV cm^{-1}. Consequently, small variations in film thickness caused by rough growth can have a large impact on device function. In particular, premature breakdown can occur at thin spots in the multiplication layer, allowing dark current to pass through the conductive microplasmas that form. Growth of smooth layers of uniform thickness is therefore essential.

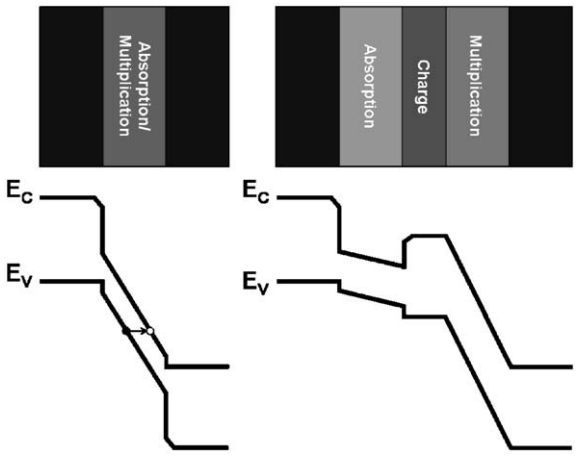

Fig. 1. Layer schematic and band edge diagram of how a SACM design (right) reduces tunneling leakage in long-wavelength APDs.

1.2. Growth mode and surface roughness

Surface morphology of unstrained thin films depends upon the relative balance between diffusive and convective mass flow during growth. Following the discussion of Tsao, growth mode can be categorized by a Peclet number expressing the ratio between step flow velocity driven by the arrival of new adatoms (convective mass flow) and the surface diffusion velocity of those adatoms [11]:

$$P = \frac{L^2 \times r}{D}, \tag{1.1}$$

where L is the average spacing between monolayer steps, r is the deposition rate in monolayers per second, and D is the surface diffusion constant.

When $P \ll 1$, diffusion dominates and growth proceeds by the step-flow mechanism in which group-III adatoms migrate to step edges, where they preferentially incorporate. Step-flow conditions produce very smooth surfaces since the adatoms tend to fill in depressions and erase irregularities. On the other hand, when $P > 1$

diffusion cannot keep pace with the arrival of new adatoms, and growth proceeds by a two-dimensional nucleation process in which the surface becomes segmented into island-like clusters which grow and coalesce. Depending upon the particulars, the islands may stay two-dimensional, periodically forming complete monolayers and preserving a smooth surface (small P), or they may pile up into three-dimensional mounds, forming a rough surface divided into a network of cells (large P). Growth mode can therefore be manipulated by controlling P: L varies with the vicinal angle of the substrate; r is controlled directly by the grower; D largely depends upon adatom lifetime and surface migration velocity (a function of substrate temperature, the bond strength of each chemical species, and arsenic overpressure).

It should be emphasized at this point that the materials in question are lattice-matched both to their substrate and to each other, so the well-known islanding mechanisms associated with growth of strained layers are not active. Except for the extreme case of arsenic deficiency, lattice-matching of AlGaInAs is insensitive to variation of arsenic overpressure and substrate temperature, as its stoichiometry is established by the group-III fluxes. Thus, it can be said with a fair degree of assurance that variations in surface morphology brought about by variations of temperature and excess arsenic pressure are dictated by the transport considerations outlined above, rather than strain effects.

1.3. The AlGaInAs material system

The AlGaInAs material system grown lattice-matched to InP bears some resemblance to the more conventional AlGaAs/GaAs material system. AlGaInAs grown by MBE is typically synthesized as a digital alloy of the two lattice-matched ternaries $In_{0.53}Ga_{0.47}As$ and $In_{0.52}Al_{0.48}As$, just as AlGaAs is commonly synthesized from the binaries GaAs and AlAs. As in the AlGaAs/GaAs material system, the aluminum-containing compound (InAlAs) forms stronger bonds and tends to grow by islanding and coalescence rather than step flow [12]. As shown in Fig. 2, this is evident from observation of reflection high-energy electron diffraction (RHEED) intensity oscillations, which cannot be seen during pure step flow growth because they originate from cycles of partial and complete monolayer coverage on the growing surface. Therefore, low adatom surface mobility and consequent three-dimensional islanding is one possible source of surface roughness in this material system. Higher substrate temperature and lower arsenic overpressure both favor smooth diffusion-driven growth because they act to increase adatom lifetime and diffusional range. Thus, InAlAs can be grown hotter than InGaAs to improve material optical quality and reduce alloy clustering [12,13]. However, the substrate

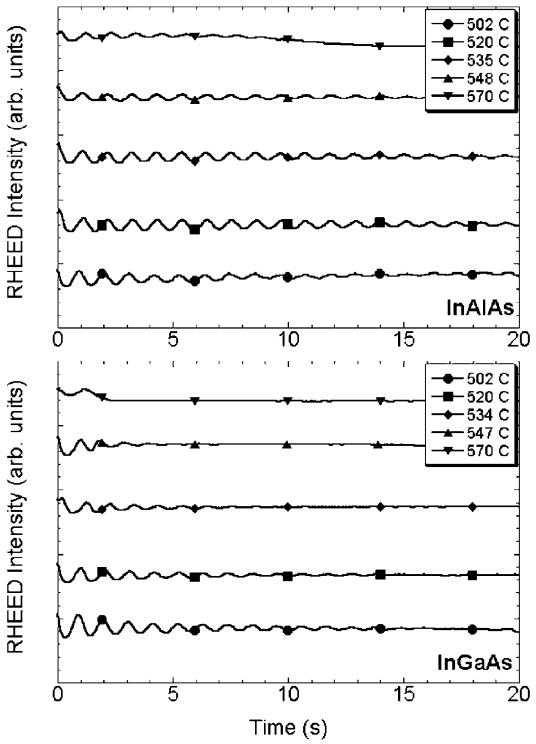

Fig. 2. RHEED intensity oscillations of InAlAs (top) and InGaAs (bottom) grown at different substrate temperatures. As the substrate temperature is raised, adatom diffusivity increases and diffusion-driven step flow growth becomes favored. The InGaAs RHEED oscillations disappear at a lower temperature than the InAlAs oscillations because InGaAs is less sticky and diffuses better at lower temperatures.

temperature and arsenic beam flux conditions which allow smooth growth are bounded by regions of the system's phase diagram in which stoichiometric AlGaInAs is no longer stable, and the growing surface decomposes into metal droplets and arsenic vapor. Thus, smooth AlGaInAs growth can only be obtained within a narrow window bounded by rough three-dimensional islanding on one side, and arsenic deficiency on the other.

2. Experimental procedure and results

The experimental work reported on in this paper was conducted in two parts. The investigation of growth conditions, growth mode, and surface morphology was based upon a set of five samples grown under varying conditions and evaluated by AFM. The relationship between surface morphology and dark current was determined by measuring the *I–V* characteristics of identical devices fabricated from five SACM APD wafers of similar design but differing roughness.

2.1. Material growth

All samples discussed in this paper were grown in a Varian Gen-II solid source MBE chamber at a rate of 1 monolayer per second on InP substrates oriented 0.5° off the (1 0 0) plane towards the (1 1 1)A plane. Lattice-matching was verified to be better than 0.16% by X-ray diffraction and growth rates were calibrated to within 1–2% by optical cavity measurements; both calibrations were tied to group-III beam fluxes to allow reproducibility from run-to-run. Substrate temperature was monitored using optical pyrometry.

Prior to growth, removal of surface oxide from the virgin substrate was accomplished by rapid heating under vacuum. Substrate temperature was ramped from 500°C to 530°C in the span of 15 s, with a minimal (10^{-6} Torr) arsenic flux supplied once the substrate passed through 520°C. Growth was initiated immediately once the substrate reached 530°C in order to minimize exchange reactions between the supplied arsenic and the phosphorus in the substrate.

2.2. Growth conditions, growth mode and surface morphology

The vicinal angle of the miscut substrates used in this study was chosen to be compatible with the epitaxial growth of InP, which was optimized in a separate investigation. Further, production of thick structures becomes impractical for growth rates much below 1 monolayer per second, so the growth rate was held constant during this study. Substrate temperature and arsenic beam flux—the two remaining levers for controlling growth

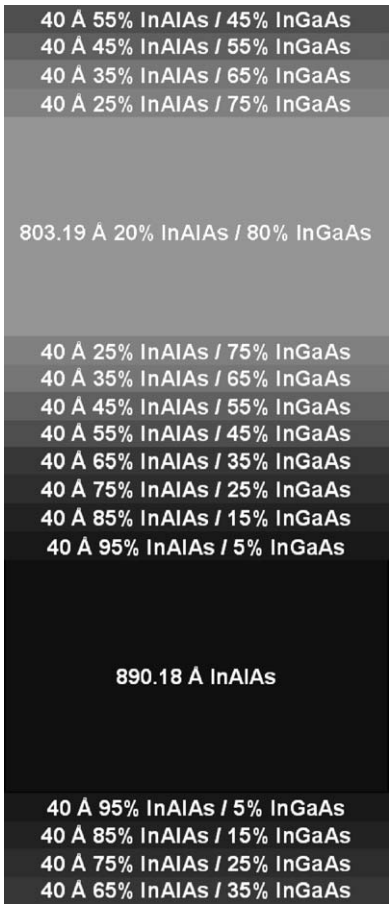

Fig. 3. Layer schematic of one DBR period appropriate for optoelectronic applications at 1550 nm.45.5 periods were grown to make the 10.5 μm structures used to investigate the relationship between growth conditions and surface morphology in very thick structures. The layers consist of pure InAlAs and $In_{0.53}Ga_{0.38}Al_{0.10}As$ with graded interfaces.

mode—were varied in order to find conditions for smooth AlGaInAs growth.

2.2.1. Sample set

Two structures were examined in this study. As shown in Fig. 3, graded 10.5 μm distributed Bragg reflectors (DBRs) of a type appropriate for optoelectronic applications at 1550 nm were grown to investigate the relationship between growth conditions and surface morphology in very thick structures. Although diffusion-driven growth tends to smooth out surface features as more material accumulates, surface roughness caused by low adatom surface mobility or arsenic deficiency tends to worsen with continued growth. Therefore, subtle differences in growth mode can more easily be detected by examining tall structures than thin ones. Past experience had indicated that optimal growth conditions for AlGaInAs on InP occur near 10^{-5} Torr of arsenic overpressure at a substrate temperature of 500°C. In order to observe the predicted marginal improvement of surface morphology with increased adatom lifetime—up to the onset of arsenic deficiency, that is—three DBR structures were grown at 500°C under arsenic beam fluxes of 4×10^{-6}, 6×10^{-6}, and 8×10^{-6} Torr. The InAlAs portions of a fourth DBR were grown at 550°C under 8×10^{-6} Torr of arsenic to test for improved morphology resulting from higher Al adatom surface mobility. The fifth structure studied, as shown in Fig. 4, was a 3 μm SACM APD wafer grown at 500°C under 1.2×10^{-5} Torr of arsenic. This last sample was grown in order to find the onset of rough three-dimensional growth caused by low adatom lifetime, the severity of which makes it detectible in shorter structures.

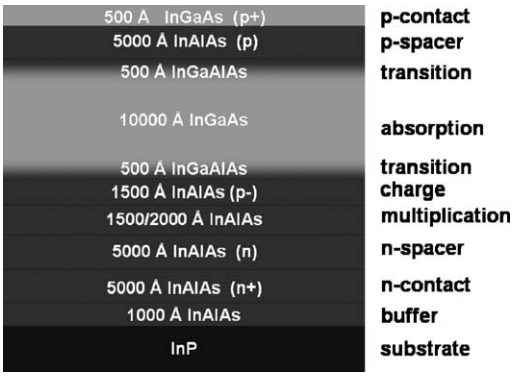

Fig. 4. APD layer schematic. The wafer grown for the growth mode study had a 2000 Å multiplication layer; the wafers grown for the dark current study had either a 1500 or 2000 Å thick multiplication layer.

2.2.2. Results

Surface roughness was extracted from AFM images of all five wafers; the results are tabulated in Table 1 and three AFM images are shown in Fig. 5a, b, and c. Optimal results were obtained from the sample grown at 500°C under 8×10^{-6} Torr of arsenic; a metal-rich polycrystalline surface was obtained from the lowest arsenic growth, whereas the highest arsenic growth gave rise to significant three-dimensional islanding.

These results illustrate two points. First, the variations of surface roughness in the structurally-identical DBR samples indicate that growth conditions—and not interfacial composition—are the origin of the observed roughness. Second, the range of observed behavior—islanding at high arsenic overpressure and faceting at low arsenic overpressure—is in keeping with what one would expect from a smooth growth window bounded by

Table 1
Growth conditions and RMS surface roughness of the samples grown to study growth mode and surface morphology

Sample	Thickness (μm)	Growth temperature (°C)	Arsenic flux (Torr)	RMS roughness (nm)
DBR	10.5	500	8×10^{-6}	1.88
DBR	10.5	500	6×10^{-6}	5.38
DBR	10.5	500	4×10^{-6}	157.78
DBR	10.5	550[a]	8×10^{-6}	9.15
APD	3	500	1.2×10^{-5}	7.06

[a] Only the InAlAs was grown at this temperature; the $In_{0.53}Ga_{0.38}Al_{0.10}As$ was grown at 500°C.

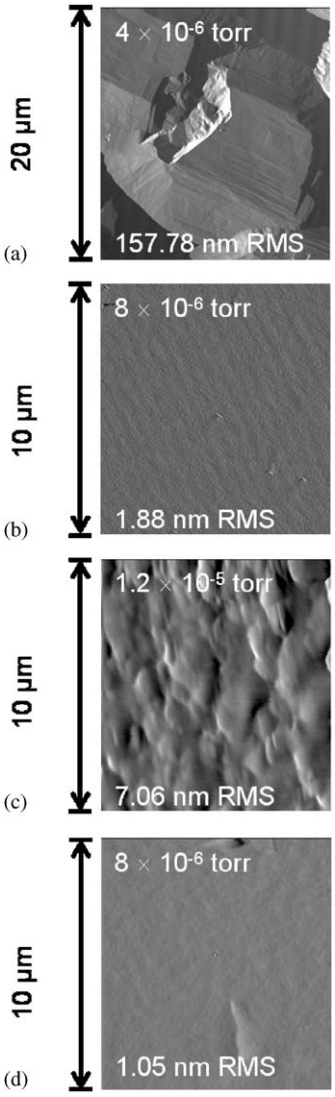

Fig. 5. AFM images of 4 samples grown at 500°C under an arsenic beam fluxes of (a) 4×10^{-6} Torr (DBR), (b) 8×10^{-6} Torr (DBR), and (c) 1.2×10^{-5} Torr (APD, sample C), and (d) 8×10^{-6} Torr (APD, sample A).

low adatom lifetime on one side and loss of stoichiometry on the other.

2.3. Surface morphology and dark current

The relationship between surface morphology and APD characteristics was investigated by studying devices fabricated from five SACM APD wafers of similar design but varying roughness. These samples were selected from a set of wafers grown in support of previously published studies, and—except for the smoothest sample—represent "failed" growths in which equipment problems allowed substrate temperature to stray outside the optimal range for the arsenic pressure used in Refs. [1,2]. Surface roughness was extracted from AFM images of the wafers.

2.3.1. Sample set

All five wafers share the layer structure shown previously in Fig. 4. Surface roughness, expressed both as an RMS value and a peak-to-peak value, are tabulated in Table 2, and AFM images of two APD wafers are shown in Fig. 5c (sample C), and 5d (sample A). Sets of 125 μm diameter APDs were fabricated from each wafer using a process described elsewhere [1]. *I–V* characteristics were measured for 15 devices from each wafer, and dark current was measured at the unity gain bias point (15 V).

2.3.2. Results

The strong dependence of dark current upon surface roughness is evident when *I–V* characteristics representative of devices fabricated from different wafers are compared side-by-side, as shown in Fig. 6. Fig. 7 is a plot of unity gain dark current against peak-to-peak roughness and reveals an exponential relationship between the two quantities, amounting to an order-of-magnitude increase for every 15 nm of roughness.

We believe that this behavior can be understood in terms of inhomogeneous breakdown: formation of microplasmas at thin areas in the multiplication region. Just as an exponential rise in current results from a linear increase in bias (and therefore field strength) in the case of a healthy APD during controlled avalanche multiplication, the premature breakdown of a small region inside an APD results in something similar when dark current is considered. Surface roughness arising from large *P* (convective growth) accumulates as growth proceeds and so is indicative of variations in layer thickness throughout the structure. Accordingly, the peak-to-peak roughness of the wafer should reflect the scale of the multiplication layer's

Table 2
Schedule of samples used in the dark current study

Sample	M-layer thickness (Å)	Peak-to-peak (nm); RMS roughness (nm)
A	2000	9.93 ; 1.05
B	2000	39.29 ; 4.86
C	2000	46.15 ; 7.06
D	1500	25.59 ; 4.40
E	1500	41.54 ; 5.19

The samples cover a broad range of roughness, and the dependence of unity gain dark current to peak-to-peak roughness is evident in Fig. 7, regardless of the difference in multiplication layer thickness.

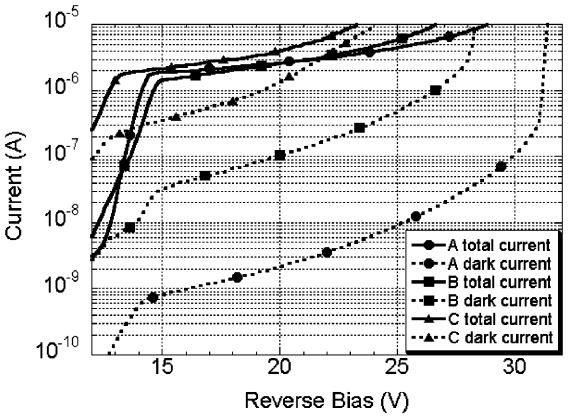

Fig. 6. *I–V* characteristics of APDs fabricated from samples A, B, and C, with differing amounts of surface roughness, as described in Table 2.

thickness variations, and in particular, its thinnest excursions. Since field strength is inversely proportional to the distance over which the potential drops inside an APD, it is sensible that dark current arising from premature breakdown should increase exponentially with a linear increase in peak-to-peak roughness.

One might object to this explanation on the grounds that surface roughness does not necessarily reflect the morphology of underlying layers. While it is true that surface roughness can arise suddenly with a change in layer composition and just as rapidly be obscured by succeeding layers, such phenomena respectively involve a sudden change in stoichiometry (lattice constant) and

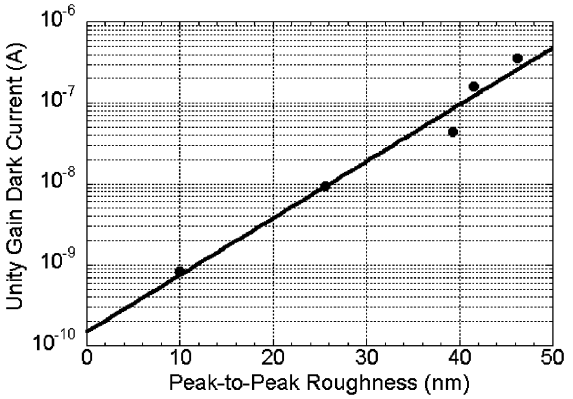

Fig. 7. Plot of unity gain dark current versus peak-to-peak roughness, revealing an exponential relationship between the two quantities. There is an order-of-magnitude increase in dark current for every 15 nm of roughness.

diffusion-dominated growth, neither of which apply in this instance. Moreover, having demonstrated control over surface roughness by means of arsenic pressure, we can be confident that the origin of the roughness lies in transport phenomena.

3. Conclusions

A narrow window for smooth AlGaInAs growth by MBE on InP has been identified and related to the mechanism of growth. Further, an empirical relationship between the surface roughness of an APD wafer as-grown and the dark current found for devices fabricated from that wafer has been discovered. Taken together, these findings constitute both a recipe for minimizing dark current in SACM APDs with thin multiplication regions, and a basis for evaluating the quality of SACM APD material prior to device fabrication and testing.

Acknowledgements

The authors wish to thank DARPA for supporting this work via CHIPS. We also want to thank the excellent laboratory support of Art Gossard, John English, and everyone else in the

UCSB MBE lab. This work made use of MRL Central Facilities supported by the MRSEC Program of the National Science Foundation under award No. DMR00-80034.

References

[1] X.G. Zheng, J.S. Hsu, X. Sun, J.B. Hurst, X. Li, S. Wang, A.L. Holmes Jr., J.C. Campbell, A.S. Huntington, L.A. Coldren, IEEE J. Quant. Electron. 38 (2002) 1536.
[2] X.G. Zheng, J.S. Hsu, J.B. Hurst, X. Li, S. Wang, X. Sun, A.L. Holmes Jr., J.C. Campbell, A.S. Huntington, L.A. Coldren, IEEE J. Quant. Electron. accepted for publication.
[3] S. Wang, J.B. Hurst, F. Ma, R. Sidhu, X. Sun, X.G. Zheng, A.L. Holmes Jr., A. Huntington, L.A. Coldren, J.C. Campbell, IEEE Photon. Technol. Lett. 14 (2002) 1722.
[4] C. Weisbuch, R. Dingle, A.C. Gossard, W. Wiegmann, Solid State Commun. 38 (1981) 709.
[5] M. Kohl, D. Heitmann, S. Tarucha, K. Leo, K. Ploog, Phys. Rev. B39 (1989) 7736.
[6] L. Gottwaldt, K. Pierz, F.J. Ahlers, E.O. Göbel, S. Nau, T. Torunski, W. Stolz, J. Appl. Phys. 94 (2003) 2464.
[7] J.N. Hollenhorst, IEEE J. Light. Technol. 8 (1990) 531.
[8] C. Lenox, H. Nie, P. Yuan, G. Kinsey, A.L. Holmes Jr., B.G. Streetman, J.C. Campbell, IEEE Photon. Technol. Lett. 11 (1999) 1162.
[9] F. Ma, S. Wang, X. Li, K.A. Anselm, X.G. Zheng, A.L. Holmes Jr., J.C. Campbell, J. Appl. Phys. 92 (2002) 4791.
[10] M.A. Saleh, M.M. Hayat, P.P. Sotirelis, A.L. Holmes Jr., J.C. Campbell, B.E.A. Saleh, M.C. Teich, IEEE Trans. Electron. Devices 48 (2001) 2722.
[11] J.Y. Tsao, Materials Fundamentals of Molecular Beam Epitaxy, Academic Press, San Diego, 1993.
[12] T.M. Brennan, J.Y. Tsao, B.E. Hammons, J.F. Klem, E.D. Jones, J. Vac. Sci. Technol. B 7 (1989) 277.
[13] D.F. Welch, G.W. Wicks, L.F. Eastman, Appl. Phys. Lett. 43 (1983) 762.